이학석사 학위논문

Effect of LOXL2 on cell viability and metastasis in NSCLC A549 cell spheroids

비소세포성 폐암 세포주 A549 spheroid에서 LOXL2가 세포의 생존과 전이에 미치는 영향

2022년 8월

서울대학교 대학원

자연과학대학 협동과정 유전공학 전공

윤 희 수

Effect of LOXL2 on cell viability and metastasis in NSCLC A549 cell spheroids

지도 교수 노 상 호

이 논문을 이학석사 학위논문으로 제출함
2022년 7월

서울대학교 대학원
자연과학대학 협동과정 유전공학 전공
윤 희 수

윤희수의 이학석사 학위논문을 인준함
2022년 8월

위 원 장 백 정 화 (인)

부위원장 노 상 호 (인)

위 원 박 한 검 (인)

Abstract

Effect of LOXL2 on cell viability and metastasis in NSCLC A549 cell spheroids

Heesu Yun

Interdisciplinary Graduate Program in Genetic Engineering

The Graduate School

Seoul National University

(Directed by Prof. Sangho Roh, D.V.M., Ph.D.)

Lung cancer is the prominent cause of cancer-associated death primarily because of distant metastatic disease. The metastatic potential of non-small cell lung cancer (NSCLC) is associated with tumor cell aggregation. However, the systemic mechanotransduction mechanism by which tumor cells dynamically aggregate and disseminate is poorly understood, especially in NSCLC. In this study, I examine whether LOXL2, a tumor

metastatic microenvironment facilitator, affects cell aggregation and plays important role in metastasis. I used poly-2-hydroxyethyl methacrylate-based 3D spheroid formation methods to mimic *in vivo* metastatic lesions. To investigate the effects of LOXL2 on A549 spheroids, A549 cells were transfected with siRNA to downregulate LOXL2 gene expression. Downregulation of LOXL2 decreased cell spheroid size and impaired compact aggregate formation in 3D culture, indicating that LOXL2 regulates spheroid-forming behavior. Furthermore, LOXL2 downregulation inhibited metastasis and induced apoptosis in A549 spheroids. Consistently, A549 cell spheroids with endogenous overexpression of LOXL2 increased metastasis. Since cell aggregation is biophysically affected in 3D culture conditions, I examined whether LOXL2 regulates cell surface matrix. As a result, knockdown of LOXL2 altered cell surface matrix and regulated the expression of glycocalyx-related genes. Overall, these data imply that LOXL2 contributes to cell surface matrix remodeling and regulates collective metastasis of free-floating aggregates.

Keywords: LOXL2, Aggregation, Apoptosis, Metastasis,NSCLC, Lung cancer, Cell surface matrix (glycocalyx)
Student Number: 2020-24033

Table of Contents

Figures

Tables

Abbreviations

NSCLC	Non-small cell lung cancers
2D	Two dimensional
3D	Three dimensional
LOXL2	Lysyl Oxidase Like 2
CTC	Circulating tumor cell
ECM	Extracellular matrix
EMT	Epithelial-to-mesenchymal transition
ICAM1	Intercellular Adhesion Molecule 1
HAPLN3	Hyaluronan And Proteoglycan Link Protein 3
GALNT4	Polypeptide N-Acetylgalactosaminyltransferase 4
GALNT3	Polypeptide N-Acetylgalactosaminyltransferase 3
HAS3	Hyaluronan Synthase 3
HSPG2	Heparan Sulfate Proteoglycan 2
GAPDH	Glyceraldehyde 3-phosphate dehydrogenase
PBS	Phosphate buffered saline
PCR	Polymerase chain reaction
Poly HEMA	poly-2-hydroxyethyl methacrylate
RT-qPCR	Quantitative real-time reverse transcription-polymerase chain reaction

RPMI	Roswell Park Memorial Institute
TEM	Transmission electron microscope

Introduction

Lung cancer is the second most common malignancy and the leading cause of mortality among tumors worldwide. Approximately 85% of all lung cancers are non-small cell lung cancer (NSCLC) [1-4]. Distant metastasis is the main cause of poor prognosis in NSCLC, with the 5-year survival rate that still remains at 19%, particularly in metastatic stage IIIA disease. Despite rapid progress in therapeutic methods and diagnostic technology, approximately 30-40% of NSCLC patients are still diagnosed at an advanced stage with adverse outcomes, making systemic therapy, including surgery, radiotherapy, and chemotherapy less effective [5,6]. Therefore, a comprehensive appreciation of the pathophysiological mechanisms of metastasis should be identified.

Cancer metastasis is a systemic succession of multiple processes, containing dissemination from the primary lesion, migration and invasion into the surrounding tissues, intravasation and survival in the circulation, and extravasation to a distant organ [7-9]. However, disseminated tumor cells are subject to continuous cellular-mechanical pressures from the tumor microenvironment [10,11]. Indeed, it is estimated that thousands of circulating tumor

cells (CTC) shed into the circulation, yet less than 0.01% of CTCs can survive and complete metastases [12]. Most tumor cells lose viability and do not survive due to detachment-induced anoikis and amorphosis, hemodynamic shear forces and attack by the immune system, leading to low success of metastasis [13-15]. Thus, survival in the circulating systems would be a limiting step in the metastatic cascade.

Recent studies have suggested that multicellular circulating tumor cells(CTC) are significantly more metastatic than individual CTCs [16-19]. Moreover, CTC clusters are associated with poorer outcomes compared to single CTC [20-23]. In support of this, several studies have reported that the formation of clusters or aggregates prevents anoikis by acquiring invasive phenotypes such as increased stem cell-like traits, evasion of natural killer cell targeting, and resistance to mechanical and metabolic stress, among others [24-26]. Therefore, the mechanism underlying by which tumor cells dynamically aggregate needs to be figured out. Although mechanistic understanding of regulating tumor cell clustering have yet to be fully elucidated, canonical cell adhesion genes including plakoglobin, ICAM1, CD54, and cadherin have been identified to mediate cluster formation [27-29]. However, a number of studies

reported that these adhesion molecule-mediated cell forces are suppressed, and the biophysical microenvironment of cell-cell interfaces is a key regulator of intercellular adhesion in advanced cancer *in vivo* [30-32]. To examine the physiological cell interaction under the *in vivo* cancer context, I used a three-dimensional (3D) cell culture on a hydrophilic poly-2-hydroxyethyl methacrylate (Poly HEMA) substrate, which mimics the clustering and dissemination of cancer cells in *in vivo* metastasis.

LOXL2 is a member of the lysyl oxidase (LOX) family, which constitutes the prototypical LOX and four related members (LOXL1-4) [33]. LOX enzymes catalyze the oxidative deamination of peptidyl lysine residues, contributing to crosslinking of extracellular matrix components, such as collagens and elastin. LOX family members, therefore, play an important role in ECM remodeling, leading to the formation of pathological tumor microenvironment [34-37]. Many studies have demonstrated an association between LOXL2 and cancer progression. High expression of LOXL2 is detected in many types of cancer and is associated with a poorer prognosis [38]. Furthermore, recent studies have shown that LOXL2 is involved in cancer cell migration,

invasion, metastasis, and epithelial–mesenchymal transition (EMT), as well as malignant transformation [39–43]. However, the role of LOXL2 in cell aggregation for survival from anoikis remains unclear. Therefore, I aimed to study the role of LOXL2 in formation of free-floating NSCLC A549 cell clusters. Furthermore, my current study is the first to indicate that LOXL2 is essential for collective metastasis by acting as a key regulator of glycocalyx network restructuring.

Materials and Methods

2.1. Cell culture and reagents

Human NSCLC A549 cells were purchased from KCLB (Seoul, Korea). Cells were in Roswell Park Memorial Institute (RPMI-1640) medium containing 10% fetal bovine serum (Gibco, Grand Island, NY, USA). Cells were maintained in a 5% CO_2 humidified atmosphere incubator at 37° C. The chemicals propylene oxide (PO), paraformaldehyde (PFA), formaldehyde (FA), and glutaraldehyde (GA) were purchased from EMS (Hatfield, PA, USA).

2.2. Poly HEMA coating

A 3% Poly HEMA (Sigma-Aldrich, St. Louis, MO, USA) solution was prepared in 95% ethanol with stirring overnight at room temperature. The Poly HEMA solution was applied on culture vessels (505 μL/36 mm diameter) in a tissue culture hood, followed by swirling in a plate rotator for 10 min. The Poly HEMA-coated vessels were left with lids covered in a laminar flow hood to prevent coffee ring effect overnight and then aseptically maintained with the lids uncovered to thoroughly dry. Poly HEMA-coated

vessels were rinsed with phosphate-buffered saline (PBS) just before use.

2.3. Spheroid aggregation assay

Following LOXL2 siRNA transfection for 24 h, 5 × 10^3 cells were plated on a Poly HEMA-coated U-bottom tissue culture 96-well plate (# 3799, Corning, Glendale, AZ, USA). Following incubation, the phenotypes of the plated cells were captured using a light microscopy.

2.4. Transient Transfection

Small interfering RNAs (siRNA) transfection of A549 cells was carried out by adding a mixture of LOXL2 siRNA or negative siRNA (OriGene, Rockville, MD, USA) and Lipofectamine™ RNAiMAX (ThermoFisher, Rockford, Il, USA) to 3 × 10^5 cells per well in 6-well plates following the manufacturer's protocol. After incubating for 24 h, cells were divided into standard tissue culture substrate (2D) and Poly HEMA-coated substrate (3D cultures). Twenty-four hours post incubating, cells were collected for further analysis. The sequences of three LOXL2 siRNA are available in Table 1. Overexpression of LOXL2 was performed by transient transfection

of pCMV-6-LOXL2 plasmid (RC200455, OriGene). pCMV6-A-Puro empty vector (PS10025, OriGene) was used as a transfection negative control.

Table 1. Sequence information on the siRNAs used in this study

Name	Sequence
siLOXL2 (1)	CUU GUU UUU CAA GAU ACU AUU AUT A
siLOXL2 (2)	GAA GAA UUA CGA GUG UGC CAA CUT C
siLOXL2 (3)	CGA UUA CUC CAA CAA CAU CAU GAA A
siNegative	CGU UAA UCG CGU AUA AUA CGC GUA T AUA CGC GUA UUA UAC GCG AUU AAC GAC

2.5. Reverse transcription quantitative real-time PCR (RT-qPCR)

Total RNA was isolated from cultured cells using a PureLink RNA Mini Kit (Invitrogen, Carlsbad, CA, USA), followed by transcription to the first-strand complementary DNA (cDNA) synthesis. RT-qPCR reactions were proceeded using a 7500 real-time PCR system (Applied Biosystems, Foster City, CA, USA). To check off-target amplifications, PCR products were subject to agarose gel and melting curve analysis. The $\Delta\Delta$CT method was employed to calculate relative expression. The expression of target mRNA was adjusted to that of internal control glyceraldehyde 3-phosphate dehydrogenase (GAPDH) in the same sample. Values are means ± SD from three separate runs performed in triplicate. The details of genes and their primers are shown in Table 2.

Table 2. List of primers used in this study

Gene	Forward sequence (5' to 3')	Reverse sequence (5' to 3')
LOXL2	TGACTGCAAGCACACGGAGGAT	TCCGAATGTCCTCCACCTGGAT
HAPLN3	TACCGCTGTGAGGTCATTGACG	CGTGGAAGTTGAACTGGTAGCG
GALNT4	GTCAAGAAGGVTCTCAGACCT	GTTCATCCTCGTTGAGCTGGAG
GALNT3	GTTGCTAGGAGCAACAGTCGC	CTGGACTTACGACAGCCGTGT
HAS3	AGCACCTTCTCGTGCATCATGC	TCCTCCAGGACTCGAAGCATCT
BCL-2	TTG TGG CCT TCT TTG AGT TCG	GGT GCC TCA GGT ACT CAG TCA
BAX	CCT GTG CAC CAA GGT GCC GGA	CCA CCC TGG TCT TGG ATC CAG
GAPDH	TGGACTCCACGACGTACTCA	ACATGTTCCAATATGATTCC

2.6 Western blot analysis

Cells were lysed with RIPA lysis buffer (Sigma-Aldrich) for 30 min on ice, and then centrifuged to clear the lysate at 13,000 *g* for 15 min at 4 ° C. Equal amounts of protein were run on SDS-PAGE and then electroblotted onto PVDF membrane (Millipore, Bedford, MA, USA). The membranes were serially probed with primary antibodies to LOXL2 (NBP1-32954, Novus Biologicals, USA) and *α*-tubulin (sc-58666, Santa Cruz Biotechnology), and, then with horseradish peroxidase (HRP)- conjugated secondary antibodies. Protein bands were detected by electrochemiluminescence (ECL) reagents (ThermoFisher).

2.7. Immunostaining

A549 cells were harvested and immunocytochemical staining was conducted. Briefly, cells washed with PBS were sequentially immersed in 4% PFA fixative (EMS) for 10 min and then in 0.15% Triton-X 100 for 5 min for permeabilization. Cells were subsequently blocked for 1 h with PBS with 3% BSA, followed by probing with primary antibody against LOXL2 overnight at 4° C. Subsequently, the cells were incubated with Alexa 488-conjugated goat anti-rabbit IgG (A-11008, Invitrogen) for 60 min at ambient

temperature, followed by labeling with rhodamine-conjugated phalloidin (Molecular Probes, Eugene, OR, USA) at a dilution of 1:2000. The cells were subsequently rinsed with PBS with tween, and placed on aseptic glass coverslips. The coverslips were immersed in a mounting medium containing 10% Mowiol 488 solution, 1 μg/mL 4′,6-diamidine-2-phenylindole dihydrochloride (DAPI; D-9542, Sigma-Aldrich), and 25% glycerol in PBS. The cells were imaged with a confocal laser scanning microscope (LSM800, Zeiss, Oberkochen, Germany).

2.8. Transmission electron microscopy of spheroids

The electron microscopy procedure used to demonstrate the glycocalyx was a slight modification of a protocol by Graham and Orenstein.[57] Briefly, cells grown in a standard tissue culture dish (2D culture) and Poly HEMA-coated dish (3D culture) were fixed in situ with freshly prepared Karnovsky's fixative containing 3% GA (EMS) and 2% FA (EMS) in 0.1M phosphate buffer, pH 7.4 with 1 mM ruthenium red (Sigma-Aldrich) for 1 h. Following fixation, cells were collected, pelleted at 50*g* centrifugation, and washed in sodium 0.1M phosphate buffer three times for 10 min each. Pellets were immersed in a secondary fixative 5% osmium tetroxide

(OsO_4) with 0.1 M ruthenium red for 3 h. Waters of post-fixed samples were serially removed with ethanol, followed by infiltration with compositions of ethanol and propylene oxide and then with compositions of PO (EMS) and Epoxy resin 812 (Sigma-Aldrich). Subsequently, samples were submerged in Epoxy resin 812 embedding medium and stuffed into an embedding enclosure to polymerize at 60 ° C for 3 days. Following the light microscope analysis of 1 μm sections stained with toluidine and sodium tetraborate, 80 nm sections cut with an EM UC7 ultra-microtome (Leica Microsystems, Wetzlar, Germany) were serially impregnated with 1% uranyl acetate solution and lead citrate on copper grids. Micrographs were captured using a JEM-1400 Flash TEM (JEOL Ltd. Japan) at 110 kV.

2.9. Spheroid 3D invasion assay

Matrigel (cat# 354232, Corning) was added to 96-well plates at 40 μl/well and solidified for 30 min at 37° C before use. Aggregates were prepared by plating cells on a Poly HEMA-coated dish for 3 h. Then, they were transferred to 96-well plates coated with Matrigel and cultured at 37° C for 24 h. Invasive sprouts were

quantified in at least 10 fields for each condition.

2.10. Transwell cell migration assay

The migration of A549 cells was investigated using a 6.5 mm Transwell with 8-μm pore size polycarbonate membrane insert (Corning). The cells were seeded on the inserts and incubated at 37 ℃. The following day, the directionally migrated cells through the inserts were immersed with 4% paraformaldehyde fixative for 15 min and stained with 0.1% crystal violet (Sigma-Aldrich) for 10 min. The inserts were washed at least three times with PBS, and non-migrated cells on the upper surface of the inserts was gently wiped away with a cotton swab. After briefly drying at room temperature, the crossed cells on the bottom surface of the insert were counted per field of view under phase-contrast microscopy.

Results

3.1. LOXL2 is involved in aggregation and spheroid formation of A549 cells

Several studies have shown that CTC clusters are significantly associated with poorer prognosis, contributing to more efficient metastasis compared to single CTCs [20-23]. I therefore investigated the role of LOXL2 in formation of cell aggregation. To this end, LOXL2 siRNA was transfected into A549 cells to knockdown expression of *LOXL2.* Knockdown of LOXL2 was confirmed by RT-qPCR and western blotting, respectively. (Fig. 1A, B). The results showed that A549 cells transfected with LOXL2 siRNA exhibited distinct morphology with decreased in size compared to the control siRNA-treated cells (Fig. 2). It was further confirmed by immunofluorescence (Fig. 3). Moreover, I found that knockdown of LOXL2 forms cells with less compact spheroid, suggesting that intercellular or interspheroid generated pulling force is weak and isotropic, compared to the control siRNA-treated cells (Fig. 4). These data suggest that downregulation of LOXL2 is critical for spheroid-forming behavior of the cell, leading to less compact spheroid and aggregation.

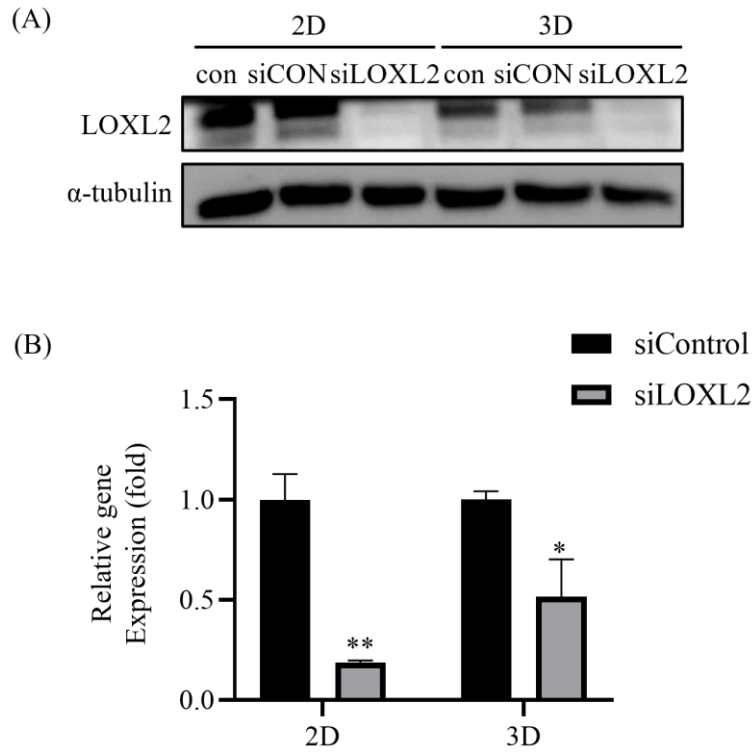

Figure 1. The expression levels of LOXL2 following *LOXL2* siRNA transfection. (A) Transient silencing of LOXL2 protein following transfection of LOXL2 siRNA. Twenty-four hours following siRNA transfection, knockdown of LOXL2 protein was validated in 2D and 3D culture conditions, respectively, by western blotting. α-tubulin was used as an internal control in western blotting. (B) Gene expression level following transfection of *LOXL2* siRNA. Twenty-four hours following siRNA transfection, knockdown of LOXL2 mRNA was validated in 2D and 3D culture conditions, respectively, by RT-qPCR. The expression of *LOXL2* transcript was normalized

to that of the GAPDH in the same cDNA sample and presented as the fold-change over that of control cells. Differences in transcript levels were evaluated for significance using two-tailed *t*-tests with unequal variance (*$P < 0.05$; $P < 0.01$; and ***$P < 0.001$).

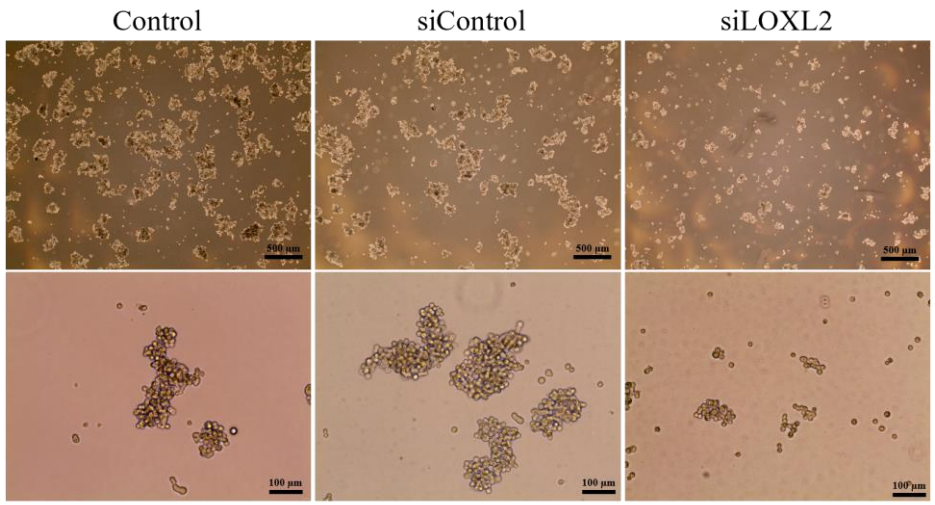

Figure 2. The phase-contrast micrographs showing the morphology of human NSCLC A549 cells grown in 3D cultures following LOXL2 siRNA transfection.

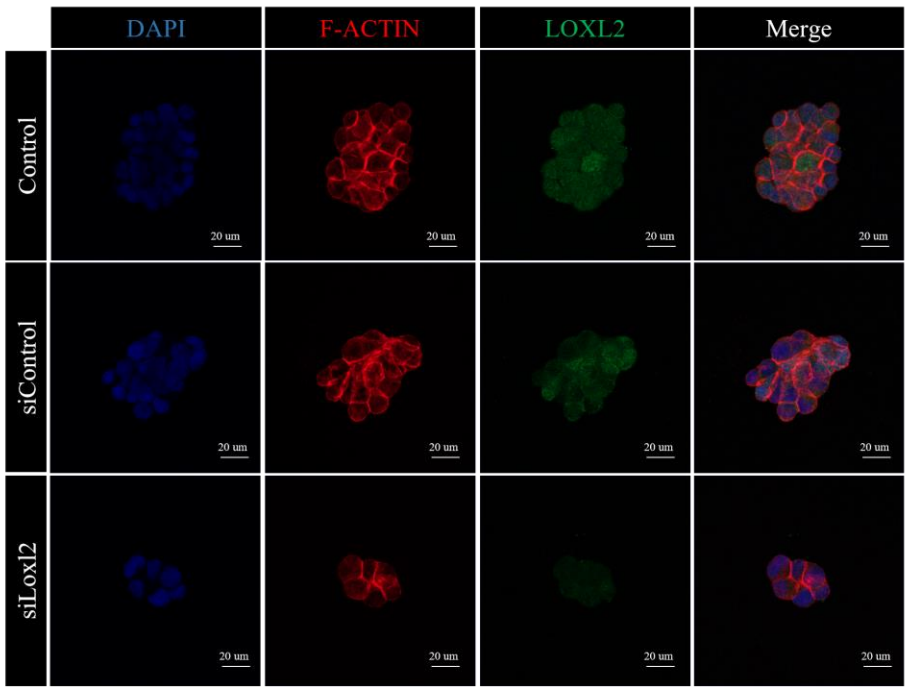

Figure 3. The immunofluorescent staining of A549 spheroids following knockdown of LOXL2. A549 cells were stained with anti-LOXL2 antibody, followed by fluorescein-conjugated antibody (green). The actin microfilaments were labeled with rhodamine-conjugated phalloidin (red), and the nuclei were counter stained with DAPI (blue).

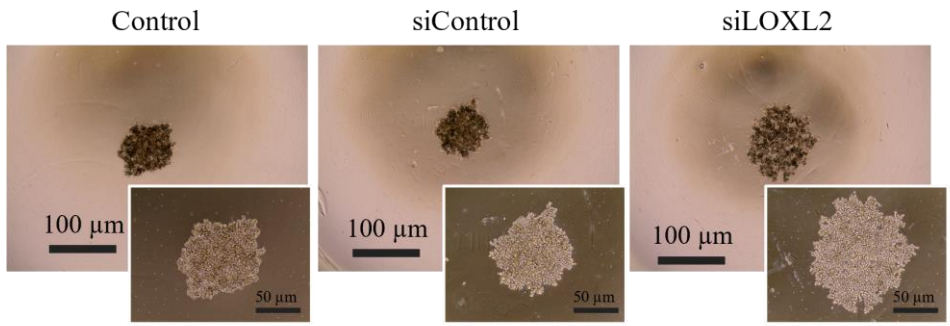

Figure 4. The effect of LOXL2 knockdown on spheroid aggregation in U-bottom 96-well tissue culture plates coated with Poly HEMA. The white box indicates enlarged images of A549 spheroids of each group.

3.2. LOXL2 controls migration and invasion in A549 cancer cell

Considering that LOXL2 is involved in cell spheroid tethering, I examined effect of LOXL2 on metastasis. The results showed that migration of A549 spheroids with reduced level with LOXL2 was decreased in a Transwell assay (Fig. 5). I next investigated whether LOXL2 expression altered A549 cancer cell invasion. To this end, I performed a 3D spheroid invasion assay in a reconstituted BM matrix. A549 cell spheroids transfected with LOXL2 siRNA exhibited less sprouting than control spheroids, indicating that downregulation of LOXL2 suppresses invasion in extracellular matrix (Fig. 6).

z

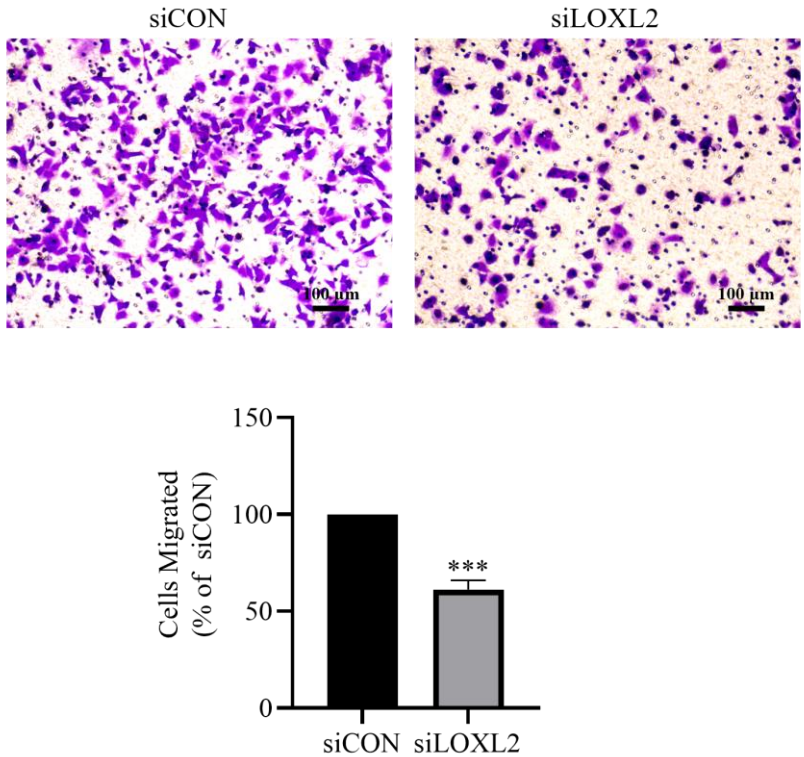

Figure 5. The representative images of the migration of NSCLC A549 spheroid transfected with siRNA LOXL2 (up) and quantification (down) in the Transwell. Twenty-four hours following siRNA transfection in 2D culture conditions, cells were further incubated in 2D and 3D culture conditions, respectively. The migration capacity of A549 spheroids with reduced level of LOXL2 was significantly lower than that of the negative control cell. $*P < 0.05$; $**P < 0.01$; and $***P < 0.001$

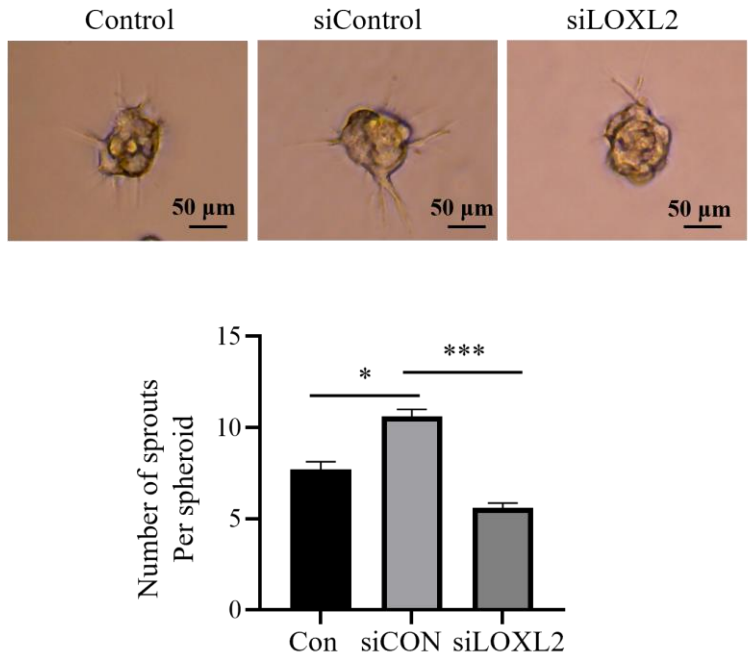

Figure 6. The representative images of invasion of A549 spheroids transfected with siRNA LOXL2 in basement membrane matrix Matrigel (up). Invasive sprouts were quantified in at least 10 fields for each condition respectively (down). $*P < 0.05$; $**P < 0.01$; and $***P < 0.001$

To confirm that these results are due to LOXL2-induced mechanism, I used a gain of function study with overexpression of LOXL2. Western blotting indicated that the expression of LOXL2 was markedly overexpressed by pCMV-6-LOXL2 plasmid (Fig. 7). The results showed that LOXL2 overexpression significantly led to increase in migration and invasion, suggesting that cells with elevated LOXL2 expression are more aggressive and have higher activity (Fig. 8, 9). Overall, these data indicate that downregulation of LOXL2 restrict the ability of A549 cancer cells to move through circulation and the stromal tissue and uncovers anti-invasive activity of LOXL2 in line with previous studies.

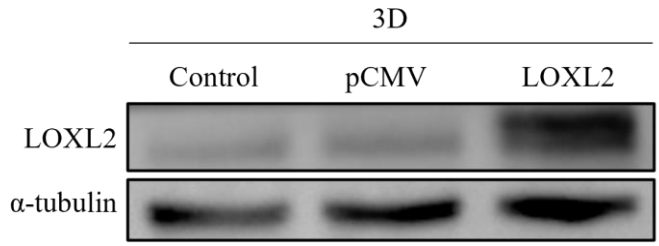

Figure 7. The protein level of 3D spheroid following pCMV-6-LOXL2 plasmid. Twenty-four hours following pCMV-6-LOXL2 and control vector pCMV-6-Puromycin transfection in 2D culture conditions, the cells were transferred to Poly HEMA 3D culture conditions. The effect of the endogenous overexpression of LOXL2 were confirmed using western blotting of cell harvest; α-tubulin was used as an internal control.

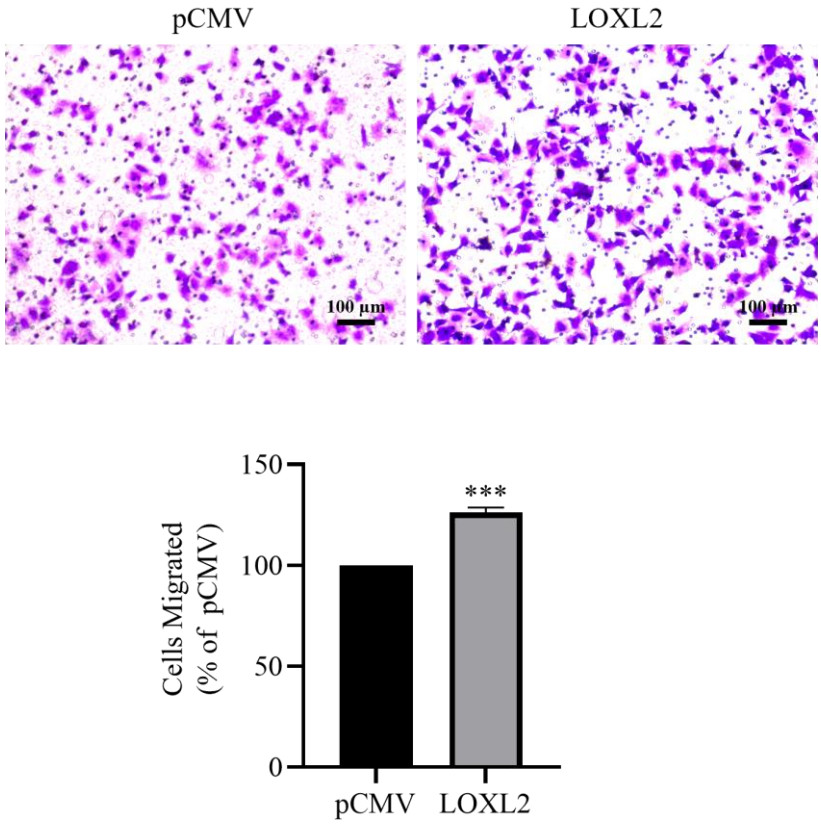

Figure 8. The representative images of the migration of NSCLC A549 spheroid transfected with pCMV-6-LOXL2 plasmid (up) and quantification (down) in the Transwell. Twenty-four hours following transfection in 2D culture conditions, cells were further incubated in 2D and 3D culture conditions, sequentially. The directional migration capacity of A549 spheroids expressing increased level of LOXL2 was significantly higher than that of the negative control cells. $*P < 0.05$; $**P < 0.01$; and $***P < 0.001$

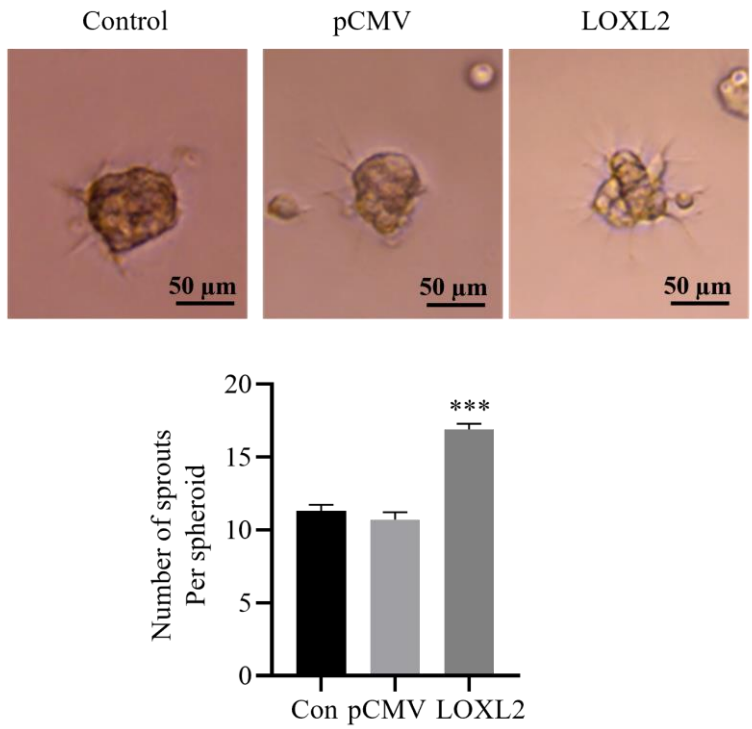

Figure 9. The representative images of invasion of A549 spheroids transfected with pCMV-6-LOXL2 plasmid in basement membrane matrix Matrigel (left). Invasive sprouts were quantified in at least 10 fields for each condition respectively (right). *P <0.05; **P < 0.01; and ***P < 0.001

3.3. Downregulation of LOXL2 leads to apoptosis in A549 spheroids

I investigated the effect of LOXL2 on cell proliferation. The results showed that downregulation of LOXL2 led to a significant decrease in cell viability compared to control siRNA (Fig. 10). Based on this observation, I further explored apoptosis related markers to evaluate mechanism of cell death. Interestingly, the results showed that the mRNA expression level of Bcl-2, an anti-apoptotic molecule, was significantly decreased and Bax, an proapoptosis molecule, was increased. Furthermore, mRNA expression of Bax/Bcl-2 ratio was also increased, which is a hallmark of apoptosis (Fig. 11). In addition, A549 spheroids with downregulated with LOXL2 exhibited increased level of proapoptotic proteins including cleaved caspase 9, cleaved caspase 3 and cleaved PARP, indicating that downregulation of LOXL2 induced apoptosis (Fig. 12).

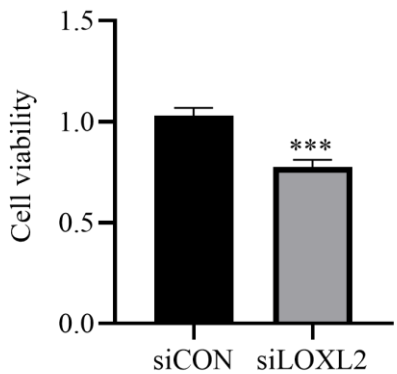

Figure 10. The cell viability of A549 spheroids following siRNA LOXL2 transfection. Twenty-four hours following transfection in 2D culture conditions, cells were further incubated in 3D culture conditions for 24h. The cell viability was investigated by WST-8 viability assay. $*P < 0.05$; $**P < 0.01$; and $***P < 0.001$

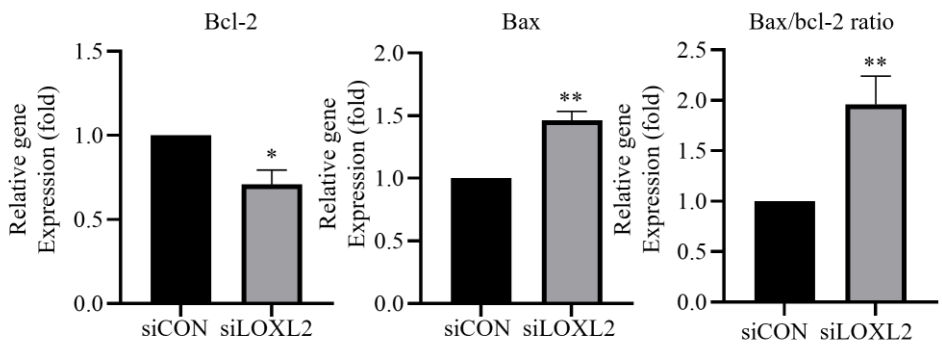

Figure 11. The mRNA expression of apoptosis genes following siLOXL2 transfection. Twenty-four hours following transfection in 2D culture conditions, cells were further incubated in 3D culture conditions for 24h. Then, cells were harvested to confirm mRNA expression related to apoptosis genes. GAPDH was used as an internal control. Differences in mRNA levels were evaluated for significance using two-tailed *t*-tests with unequal variance (*P <0.05; **P < 0.01; and ***P < 0.001).

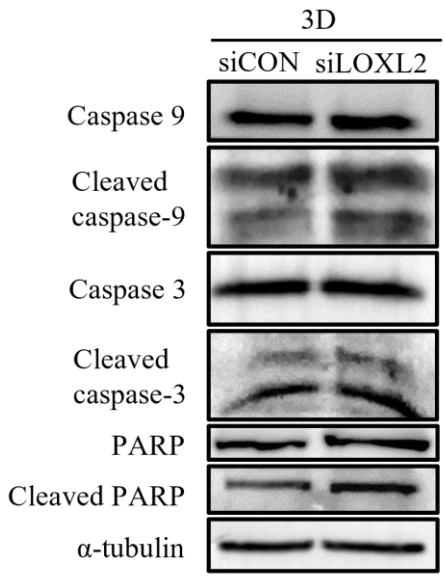

Figure 12. The effects of LOXL2 knockdown on the apoptosis signaling pathway. Twenty-four hours following transfection in 2D culture conditions, cells were further incubated in 3D culture conditions for 24h. Then, cells were harvested to confirm protein expression related to apoptosis genes using Western blotting. α-tubulin was used as an internal control.

3.4. LOXL2 may regulate cell adhesion through glycocalyx

My results showed that LOXL2 expression regulates formation of clustering, leading to collective metastasis. Here, I examined the possibility that glycocalyx is a target of LOXL2 because one of the factors regulating biophysical feature of cell–cell interfaces is glycocalyx which is found on the surface of cell with dense, charged and hydrated nature of its main components, acting as a repulsive barrier. To investigate this hypothesis directly, I analyzed the glycocalyx using transmission electron microscopy (TEM). Interestingly, morphology of glycocalyx was altered upon knockdown of endogenous LOXL2 expression. The glycocalyx in A549 cells with transfected with LOXL2 siRNA was more dense and shorter compared with control A549 cells (Fig. 13).

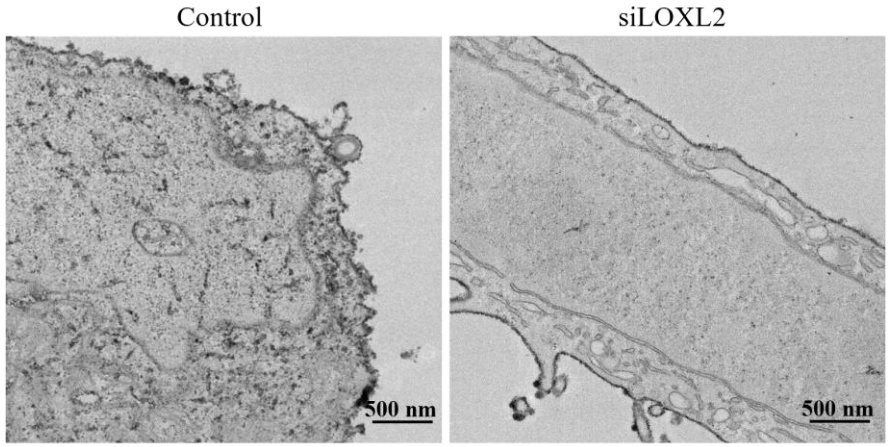

Figure 13. The effects of LOXL2 knockdown with siRNA on cell surface remodeling (glycocalyx) in 2D adhesive culture. Representative transmission electron microscopy (TEM) micrographs of NSCLC A549 cells showing glycoconjugates of glycocalyx in control (left panel) and LOXL2 siRNA-treated cells (right panel). Images were captured after 24 h of culture using polycationic ruthenium red as a stain for TEM.

Furthermore, I examined whether glycocalyx expression is altered upon knockdown of LOXL2 expression. To this end, I investigated a few components of glycocalyx which is known to involved in both cell adhesion and metastasis. It was observed that A549 spheroids with reduced level of LOXL2 exhibited the increase in expression of GALNT3 and GALNT4, tumor suppressors, and the decrease in expression of HAPLN3 and HSPG2 in 3D culture (Fig. 14). To confirm regulation of glycocalyx expression is due to LOXL2, I also analyzed the glycocalyx expression following LOXL2 overexpression. The results showed that expression levels of genes except for HAPLN3 were downregulated (Fig. 15). Furthermore, the expression level of HSPG2 showed same tendency both in downregulation and upregulation of LOXL2 level. Therefore, GALNT3 and GALNT4 could be a target of glycocalyx affected by LOXL2. Together, these results led me to conclude that LOXL2 regulates glycocalyx and affects the expression of the components constituting glycocalyx.

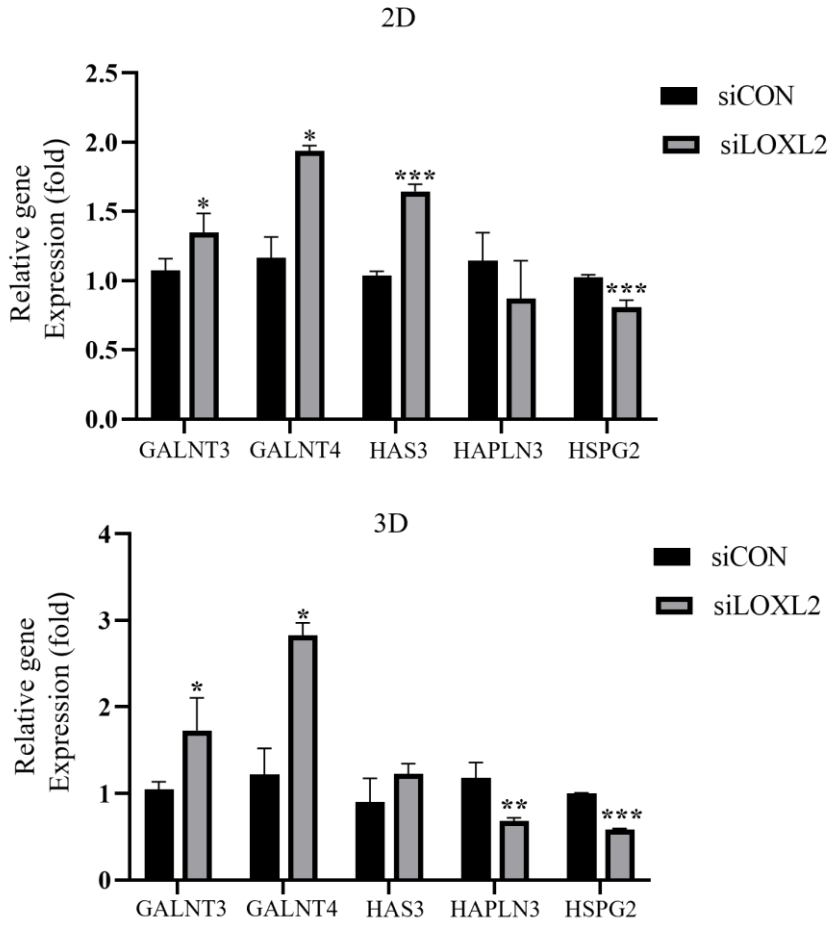

Figure 14. The expression level of glycocalyx-related gene in 2D (up) and 3D (down) cells following LOXL2 knockdown. The mRNA level was normalized to that of the GAPDH in the same cDNA sample and presented as the fold-change over that of control cells. Differences in mRNA levels were evaluated for significance using two-tailed *t*-tests with unequal variance (*P <0.05; **P < 0.01; and ***P < 0.001).

3D

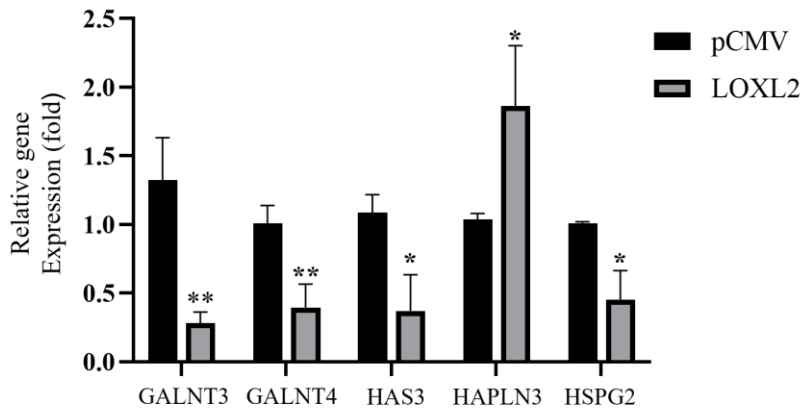

Figure 15. The expression level of glycocalyx-related gene on A549 spheroid following LOXL2 overexpression. The mRNA level was normalized to that of the GAPDH in the same cDNA sample and presented as the fold-change over that of control cells. Differences in mRNA levels were evaluated for significance using two-tailed *t*-tests with unequal variance (*P <0.05; **P < 0.01; and ***P < 0.001).

Discussion

In this study, I found that LOXL2 expression contributes to A549 cancer cell clustering and regulates collective metastasis of substratum-detached cells. This finding has important implications for understanding of tumor biology and translation to therapeutic control in NSCLC metastasis.

The ability of forming clustering plays important role in survival in anchorage-independent conditions, characteristics of circulating systems. My study demonstrated that LOXL2 expression contributes to tumor cell clustering. LOXL2 is known to promote migration and invasion through remodeling surrounding ECM [44]. However, the mechanism underlying LOXL2-mediated metastasis is limited in 2D adhesive culture conditions. Moreover, recent study revealed that elevated expression of LOXL2 associates with poor prognosis in non-small lung cancer [45]. Indeed, my results showed that downregulation of LOXL2 blocks tumor cell cluster formation, thereby inhibiting metastasis and anti-apoptosis. In support of this, several studies have suggested that size and compaction of spheroid is associated with invasive phenotypes [46,47]. Therefore, my study is the first to indicate LOXL2 is essential for collective metastasis through regulating cell-cell

adhesion under anchorage-independent conditions.

The cell viability of A549 spheroid following siLOXL2 transfection was decreased. I further explored mechanism of cell death using apoptosis markers. Apoptosis is programmed cell death characterized by shrinkage of the cell, chromatin condensation, fragmentation of DNA, membrane blebbing. The apoptosis pathway starts from increasing expression of BAX, proapoptotic molecules, and releasing cytochrome c from mitochondrial outer membrane. Then, the released cytochrome c activates inactive form of proteins including caspase 9, caspase 3, PARP, consequently leading to apoptosis [48,49]. My study showed that downregulation of LOXL2 activates caspases, leading to increased expression of active form of caspases such as cleaved caspase 9, cleaved caspase 3 and cleaved PARP. Therefore, my study demonstrated that knockdown of LOXL2 induces apoptosis in A549 spheroids, which could be referred to as anoikis.

Cell-cell adhesion is not only mediated through surface expression of specific receptors, but also by glycoconjugate glycocalyx, a ubiquitous carbohydrate-enriched sugar surface coating of glycolipids, glycoproteins, and glycosaminoglycans [50,51]. Matthew J. Paszek reported that glycocalyx with high o-

glycan content promotes cell survival in a suspended state [49]. This data suggested that glycocalyx not only mediate cell adhesion but also critical for cell survival following cell detachment. In regard to the mechanisms of action involving LOXL2, I hypothesized that LOXL2 catalyzes the core protein of glycocalyx, resulting in inter- or intra-crosslinking, and the enzymatic activity of LOXL2 has been studied extensively in ECM cross-linking. However, intracellular functions have been described more extensively for LOXL2. LOXL2 coordinates with transcription factors to regulate the expression of genes including ACAN, SOX2, and CDH1 [41,52,53]. However, my study is limited to providing that LOXL2 affects structure and expression of several components of glycocalyx, but specific target is not discovered. Indeed, many studies investigated role of glycocalyx on cancer progression by manipulating individual components of glycocalyx since each of them functions differently [54-57]. Therefore, further research is needed to investigate by which LOXL2 changes the cell surface through either gene expression or enzyme activity, or both. It will be interesting to discover how LOXL2 remodels the cell surface.

References

1. Ferlay J, Shin HR, Bray F, Forman D, Mathers C, Parkin DM. Estimates of worldwide burden of cancer in 2008: GLOBOCAN 2008. Int J Cancer 2010;127:2893-917.
2. Jemal A, Siegel R, Ward E, Hao Y, Xu J, Thun MJ. Cancer statistics, 2009. CA Cancer J Clin 2009;59:225-49.
3. Herbst RS, Morgensztern D, Boshoff C. The biology and management of non-small cell lung cancer. Nature 2018;553:446-54.
4. Herbst RS, Heymach JV, Lippman SM. Lung cancer. N Engl J Med 2008;359:1367-80.
5. Walder D, O'Brien M. Looking back and to the future: Are we improving 'cure' in non-small cell lung cancer? Eur J Cancer 2017;75:192-4.
6. Yano T, Okamoto T, Fukuyama S, Maehara Y. Therapeutic strategy for postoperative recurrence in patients with non-small cell lung cancer. World J Clin Oncol 2014;5:1048-54.
7. Steeg PS. Targeting metastasis. Nat Rev Cancer 2016;16:201-18.
8. Altorki NK, Markowitz GJ, Gao D, et al. The lung microenvironment: an important regulator of tumour growth and metastasis. Nat Rev Cancer 2019;19:9-31.
9. Turajlic S, Swanton C. Metastasis as an evolutionary process. Science 2016;352:169-75.
10. Mehlen P, Puisieux A. Metastasis: a question of life or death. Nat Rev Cancer 2006;6:449-58.
11. Riggio AI, Varley KE, Welm AL. The lingering mysteries of metastatic recurrence in breast cancer. Br J Cancer 2021;124:13-26.
12. Joyce, J. A. and J. W. Pollard. Microenvironmental regulation of metastasis.Nat Rev Cancer 2009; 9(4): 239-252.
13. Taddei ML, Giannoni E, Fiaschi T, Chiarugi P (2012) Anoikis: an emerging hallmark in health and diseases. *J Pathol* 2012; 226 (2): 380–393
14. Mehlen P, Puisieux A. Metastasis: a question of life or death. Nat Rev Cancer 2006;6:449-58.
15. Buchheit CL, Weigel KJ, Schafer ZT. Cancer cell survival during

detachment from the ECM: multiple barriers to tumour progression. Nat Rev Cancer 2014;14:632-41.
16. Aceto N, Bardia A, Miyamoto DT, et al. Circulating tumor cell clusters are oligoclonal precursors of breast cancer metastasis. Cell 2014;158:1110-22.
17. Gkountela S, Castro-Giner F, Szczerba BM, et al. Circulating Tumor Cell Clustering Shapes DNA Methylation to Enable Metastasis Seeding. Cell 2019;176:98-112 e14.
18. Labuschagne CF, Cheung EC, Blagih J, Domart MC, Vousden KH. Cell Clustering Promotes a Metabolic Switch that Supports Metastatic Colonization. Cell Metab 2019;30:720-34 e5.
19. Min S, Choe C, Roh S. AQP3 Increases Intercellular Cohesion in NSCLC A549 Cell Spheroids through Exploratory Cell Protrusions. Int J Mol Sci 2021;22.
20. Aceto, N. et al. Circulating tumor cell clusters are oligoclonal precursors of breast cancer metastasis. *Cell* 2014;158, 1110–1122
21. Aceto, N., Toner, M., Maheswaran, S. & Haber, D. A. En route to metastasis: circulating tumor cell clusters and epithelial-to-mesenchymal transition. *Trends Cancer* 2015;1, 44–52
22. Grillet, F. et al. Circulating tumour cells from patients with colorectal cancer have cancer stem cell hallmarks in ex vivo culture. *Gut* 2017; 66, 1802–1810
23. Massagué, J. & Obenauf, A. C. Metastatic colonization by circulating tumour cells. *Nature* 2016; 529, 298–306
24. Bonnet J, Rigal L, Mondesert O, et al. Mitotic arrest affects clustering of tumor cells. Cell Div 2021;16:2.
25. Donato C, Kunz L, Castro-Giner F, et al. Hypoxia Triggers the Intravasation of Clustered Circulating Tumor Cells. Cell Rep 2020;32:108105.
26. Giampieri S, Manning C, Hooper S, Jones L, Hill CS, Sahai E. Localized and reversible TGFbeta signalling switches breast cancer cells from cohesive to single cell motility. Nat Cell Biol 2009;11:1287-96.
27. Padmanaban V, Krol I, Suhail Y, et al. E-cadherin is required for metastasis in multiple models of breast cancer. Nature 2019;573:439-44.
28. Campbell K, Casanova J. A role for E-cadherin in ensuring

cohesive migration of a heterogeneous population of non-epithelial cells. Nat Commun 2015;6:7998.
29. Schuster E, Taftaf R, Reduzzi C, Albert MK, Romero-Calvo I, Liu H. Better together: circulating tumor cell clustering in metastatic cancer. Trends Cancer 2021;7:1020-32.
30. Belardi B, Son S, Felce JH, Dustin ML, Fletcher DA. Cell-cell interfaces as specialized compartments directing cell function. Nat Rev Mol Cell Biol 2020;21:750-64.
31. Chin-Hun Kuo J, Gandhi JG, Zia RN, Paszek MJ. Physical biology of the cancer cell glycocalyx. Nat Phys 2018;14:658-69.
32. Abduljauwad SN, Ahmed HU, Moy VT. Melanoma treatment via non-specific adhesion of cancer cells using charged nano-clays in pre-clinical studies. Sci Rep 2021;11:2737.
33. Barker HE, Cox TR, Erler JT. The rationale for targeting the LOX family in cancer. Nat Rev Cancer 2012;12:540-52.
34. Zhang, X., et al. Crystal structure of human lysyl oxidase-like 2 (hLOXL2) in a precursor state.Proc Natl Acad Sci U S A 2018; 115(15): 3828-3833.
35. Wong CC, Tse AP, Huang YP, Zhu YT, Chiu DK, Lai RK, Au SL, Kai AK, Lee JM, Wei LL, et al: Lysyl oxidase-like 2 is critical to tumor microenvironment and metastatic niche formation in hepatocellular carcinoma
36. Xiao, Q. and G. Ge. Lysyl oxidase, extracellular matrix remodeling and cancer metastasis. Cancer Microenviron 2012; 5(3): 261-273.
37. Barry-Hamilton V, Spangler R, Marshall D, et al. Allosteric inhibition of lysyl oxidase-like-2 impedes the development of a pathologic microenvironment. Nat Med 2010;16:1009-17.
38. Wu L and Zhu Y. The function and mechanisms of action of LOXL2 in cancer (Review). Int J Mol Med. 2015; 36:1200–1204.
39. Xu XH, Jia Y, Zhou X, et al. Downregulation of lysyl oxidase and lysyl oxidase-like protein 2 suppressed the migration and invasion of trophoblasts by activating the TGF-beta/collagen pathway in preeclampsia. Exp Mol Med 2019;51:1-12.
40. Moreno-Bueno G, Salvador F, Martin A, et al. Lysyl oxidase-like 2 (LOXL2), a new regulator of cell polarity required for metastatic dissemination of basal-like breast carcinomas. EMBO Mol Med 2011;3:528-44.
41. Tashkandi MM, Alsaqer SF, Alhousami T, et al. LOXL2 promotes

aggrecan and gender-specific anabolic differences to TMJ cartilage. Sci Rep 2020;10:20179.
42. Cuevas, E. P., et al. LOXL2 drives epithelial-mesenchymal transition via activation of IRE1-XBP1 signalling pathway. Sci Rep 2017; 7: 44988.
43. Hong, X. and J. J. Yu. Silencing of lysyl oxidaselike 2 inhibits the migration, invasion and epithelial to mesenchymal transition of renal cell carcinoma cells through the Src/FAK signaling pathway. Int J Oncol 2019; 54(5): 1676-1690.
44. Dinca, S. C., et al. Novel mechanism for OSM-promoted extracellular matrix remodeling in breast cancer: LOXL2 upregulation and subsequent ECM alignment. Breast Cancer Res 2021; 23(1): 56.
45 Zhan, P., et al. Increased lysyl oxidase-like 2 associates with a poor prognosis in non-small cell lung cancer. Clin Respir J 2018; 12(2): 712-720.
46. Gunay, G., et al. The effects of size and shape of the ovarian cancer spheroids on the drug resistance and migration. Gynecol Oncol 2020;159(2): 563-572.
47. Sodek, K. L., et al. Compact spheroid formation by ovarian cancer cells is associated with contractile behavior and an invasive phenotype." Int J Cancer 2009. 124(9): 2060-2070.
48. Jan, R. and G. E. Chaudhry. Understanding Apoptosis and Apoptotic Pathways Targeted Cancer Therapeutics. AdvPharm Bull 2019; 9(2): 205-218.
49. Khan, S. U., et al. Understanding the cell survival mechanism of anoikis-resistant cancer cells during different steps of metastasis. Clin Exp Metastasis. 2022
50. Shurer CR, Kuo JC, Roberts LM, et al. Physical Principles of Membrane Shape Regulation by the Glycocalyx. Cell 2019;177:1757-70 e21.
51. Paszek MJ, DuFort CC, Rossier O, et al. The cancer glycocalyx mechanically primes integrin-mediated growth and survival. Nature 2014;511:319-25
52. Shurer, C. R., et al. Genetically Encoded Toolbox for Glycocalyx Engineering: Tunable Control of Cell Adhesion, Survival, and Cancer Cell Behaviors. ACS Biomater Sci Eng 2018; 4(2): 388-399.
53. Iturbide A, Pascual-Reguant L, Fargas L, et al. LOXL2 Oxidizes Methylated TAF10 and Controls TFIID-Dependent Genes during

Neural Progenitor Differentiation. Mol Cell 2015;58:755-66.
54. Herranz N, Dave N, Millanes-Romero A, et al. Lysyl oxidase-like 2 (LOXL2) oxidizes trimethylated lysine 4 in histone H3. FEBS J 2016;283:4263-73.
55. Guedan, S., et al. Hyaluronidase expression by an oncolytic adenovirus enhances its intratumoral spread and suppresses tumor growth.Mol Ther 2010;18(7): 1275-1283
56. Offeddu, G. S., et al. The cancer glycocalyx mediates intravascular adhesion and extravasation during metastatic dissemination. Commun Biol 2021;4(1): 255.
57. Reitsma, S., et al. The endothelial glycocalyx: composition, functions, and visualization. Pflugers Arch 2007; 454(3): 345-359.

국문초록

비소세포성 폐암 세포주 A549 spheroid에서 LOXL2가 세포의 생존과 전이에 미치는 영향

윤 희 수
협동과정 유전공학 전공
서울대학교 대학원
(지도교수: 노상호, D.V.M., Ph.D.)

폐암에서 전이는 사망의 주요 원인이다. 이러한 비소세포성 폐암(NSCLC)의 전이는 종양세포의 응집과 밀접하게 연관이 있다. 하지만, 기계역학적 관점에서 종양세포의 응집에 대한 연구는 드물게 보고되었다. 따라서 본 연구에서 LOXL2 유전자가 세포 응집에 중요한 역할을 하는지에 대한 여부를 확인하였다. 생체 내의 전이 환경을 모방하기 위하여 poly-2-hydroxyethyl methacrylate 기반의 3차원 배양방법을 사용하였다. 전이 촉진 유전자인 LOXL2의 발현을 감소시켰을 때, 밀집도가 낮은 응집체를 형성하는 것을 확인함으로써 LOXL2가 세포 응집을 조절한다는 것을 확인하였다. 또한, LOXL2 발현의 감소는 세포의 이동과 침습성을 억제하였고 세포의 생존 또한 감소시키는 것을 확인하였다. 이러한

성장의 억제는 세포사멸 관련 유전자를 통하여 세포사멸사에 기인한 것이라는 것을 확인하였다. 반면에, LOXL2의 과발현은 이동과 침습성을 증가시키는 것을 확인하였다. 지지체 비의존성 환경에서 세포의 응집은 생물물리학적 영향을 받기 때문에, 이를 조절하는 것으로 알려진 세포 표면 매트릭스 (글리코카릭스) 와 LOXL2 간의 연관성에 대하여 조사하였다. 그 결과, LOXL2의 감소는 형태학적으로 세포 표면 매트릭스를 변형시켰고 매트릭스를 구성하는 요소들의 발현량 또한 조절하는 것을 확인하였다. 종합적으로, 본 연구는 부유 환경에서 LOXL2가 종양 세포의 세포 표면 매트릭스를 조절하고 세포의 응집에 관여하여 암의 진행에 영향을 미침을 밝혀내었다.

주요어: LOXL2, 응집, 세포자연사, 종양의 전이, 비소세포성 폐암, 폐암, 세포 표면 매트릭스(글리코카릭스)

학번: 2020-24033